

Electric-field control of phase separation and memory effect in $\text{Pr}_{0.6}\text{Ca}_{0.4}\text{MnO}_3/\text{Pb}(\text{Mg}_{1/3}\text{Nb}_{2/3})_{0.7}\text{Ti}_{0.3}\text{O}_3$ heterostructures

Q. P. Chen, J. J. Yang, Y. G. Zhao, S. Zhang, J. W. Wang et al.

Citation: *Appl. Phys. Lett.* **98**, 172507 (2011); doi: 10.1063/1.3584025

View online: <http://dx.doi.org/10.1063/1.3584025>

View Table of Contents: <http://apl.aip.org/resource/1/APPLAB/v98/i17>

Published by the [American Institute of Physics](#).

Related Articles

Reduced leakage currents and possible charge carriers tuning in Mg-doped $\text{Ga}_{0.6}\text{Fe}_{1.4}\text{O}_3$ thin films
Appl. Phys. Lett. **100**, 262904 (2012)

Variation of ferroelectric properties in $(\text{Bi,Pr})(\text{Fe,Mn})\text{O}_3/\text{SrRuO}_3\text{-Pt}/\text{CoFe}_2\text{O}_4$ layered film structure by applying direct current magnetic field
J. Appl. Phys. **111**, 124103 (2012)

Observation of strong magnetoelectric effects in $\text{Ba}_{0.7}\text{Sr}_{0.3}\text{TiO}_3/\text{La}_{0.7}\text{Sr}_{0.3}\text{MnO}_3$ thin film heterostructures
J. Appl. Phys. **111**, 104104 (2012)

Magnetodielectric effect in CdS nanosheets grown within Na-4 mica
J. Appl. Phys. **111**, 074303 (2012)

Piezoresponse force microscopy and vibrating sample magnetometer study of single phased Mn induced multiferroic BiFeO_3 thin film
J. Appl. Phys. **111**, 064110 (2012)

Additional information on *Appl. Phys. Lett.*

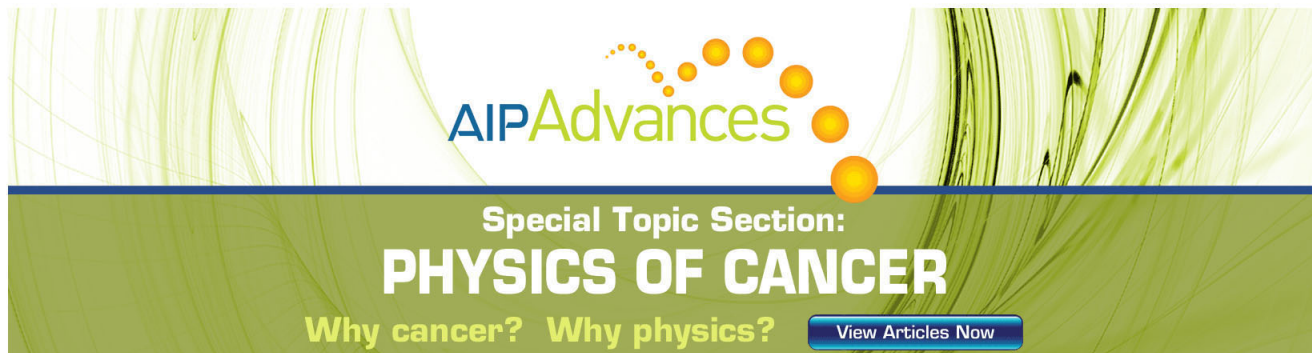
Journal Homepage: <http://apl.aip.org/>

Journal Information: http://apl.aip.org/about/about_the_journal

Top downloads: http://apl.aip.org/features/most_downloaded

Information for Authors: <http://apl.aip.org/authors>

ADVERTISEMENT



AIP Advances

Special Topic Section:
PHYSICS OF CANCER

Why cancer? Why physics? [View Articles Now](#)

Electric-field control of phase separation and memory effect in $\text{Pr}_{0.6}\text{Ca}_{0.4}\text{MnO}_3/\text{Pb}(\text{Mg}_{1/3}\text{Nb}_{2/3})_{0.7}\text{Ti}_{0.3}\text{O}_3$ heterostructures

Q. P. Chen,¹ J. J. Yang,¹ Y. G. Zhao,^{1,a)} S. Zhang,¹ J. W. Wang,¹ M. H. Zhu,¹ Y. Yu,² X. Z. Zhang,² Zhu Wang,³ Bin Yang,³ D. Xie,⁴ and T. L. Ren⁴

¹Department of Physics and The Key Laboratory of Atomic and Nanosciences, Ministry of Education, Tsinghua University, Beijing 100084, People's Republic of China

²Department of Materials Science and Engineering, Laboratory of Advanced Materials, Beijing National Center for Electron Microscopy, Tsinghua University, Beijing 100084, People's Republic of China

³Department of Physics, Harbin Institute of Technology, Harbin 150080, People's Republic of China

⁴Institute of Microelectronics and Tsinghua National Laboratory for Information Science and Technology (TNList), Tsinghua University, Beijing 100084, People's Republic of China

(Received 28 March 2011; accepted 6 April 2011; published online 29 April 2011)

Heterostructures were fabricated by growing $\text{Pr}_{0.6}\text{Ca}_{0.4}\text{MnO}_3$ (PCMO) films on $\text{Pb}(\text{Mg}_{1/3}\text{Nb}_{2/3})_{0.7}\text{Ti}_{0.3}\text{O}_3$ substrates. It was shown that the magnetizations of the samples can be tuned dramatically by electric fields via piezostain and the effect is dominated by the change in phase separation. More interestingly, the electric-field control of magnetization is nonvolatile, manifesting a memory effect of strain. The results were discussed by considering the effect of electric-field-induced strain on the energy landscape of PCMO and the resultant change in phase separation. This work is helpful for exploring the evolution of phase separation with well-controlled strains and the magnetoelectric coupling effect. © 2011 American Institute of Physics.

[doi:10.1063/1.3584025]

Heterostructures composed of magnetic (M) and ferroelectric (FE) materials have attracted much attention due to their importance in exploring the magnetoelectric (ME) coupling effect.¹⁻⁹ One of the key issues in the study of M/FE heterostructures is the electric-field control of magnetization. There have been some reports on this topic in various M/FE heterostructures,^{1-3,5-7} however, the electric-field control of magnetization in the M/FE heterostructures is still limited for the phase separated manganites,^{8,9} which exhibit a variety of exotic behaviors.¹⁰ It was assumed that the electric-field control of magnetization in the M/FE heterostructures composed of the phase separated manganites is due to the change in phase separation,^{8,9} however, it is not conclusive since only the in-plane magnetization was measured. It has been shown through the measurement of magnetizations along both the in-plane and out-of-plane directions that the electric-field-induced change in magnetic anisotropy plays an important role in the electric-field control of magnetization in the M/FE heterostructures.⁶ More importantly, there has been no report on the memory effect of the electric-field control of magnetization in the M/FE heterostructures composed of the phase separated manganites. $\text{Pr}_{0.6}\text{Ca}_{0.4}\text{MnO}_3$ (PCMO) is an interesting phase separated manganite with a coexistence of ferromagnetic (FM) and charge-ordered antiferromagnetic (COAFM) phases in a wide temperature range¹¹ while $\text{Pb}(\text{Mg}_{1/3}\text{Nb}_{2/3})_{0.7}\text{Ti}_{0.3}\text{O}_3$ (PMN-PT) is a well-known FE material with an excellent piezoelectric property. In the PCMO/PMN-PT heterostructures, the strain transferred to the PCMO films can be modulated continuously and reversibly. This continuity and reversibility with moderate strains, which cannot be realized in the previous studies of strain effect on the phase separation of manganites via different substrates,¹²⁻¹⁴ provides a good opportunity to study the ef-

fect of strain on the evolution of phase separation of manganites with well-controlled strains. So far there is no report on the electric-field control of magnetization in the PCMO/FE heterostructures. In this letter, we report on the fabrication of the PCMO/PMN-PT heterostructures, dramatic change in magnetization induced by electric fields and memory effect of ME coupling or strain. We demonstrated that the electric-field control of magnetization is dominated by the change in phase separation in PCMO. The results were discussed in terms of the strain induced change in phase separation with the energy landscape scenario.

PCMO thin films were deposited on one-side-polished (001)-oriented PMN-PT single-crystal substrates by pulsed laser deposition. During deposition, the temperature of the substrate was kept at 700 °C with a 40 Pa oxygen pressure. The film thickness is about 300 nm. X-ray diffraction (XRD) patterns of the samples were obtained using a Rigaku D/max-RB x-ray diffractometer with a $\text{Cu } K_\alpha$ radiation. A JEM-2010F (200 kV) transmission electron microscope (TEM) was used for the microstructure analysis. The morphology of the films was measured using a Nanoscope IIIa Dimension 3100 atomic force microscope. Au was deposited on the full area of the film and the back of PMN-PT as electrodes. Au on PCMO is defined as the positive electrode. The voltage was applied *in situ* across the PCMO/PMN-PT heterostructure by a Keithley 6517A electrometer and the current is below 5 nA. The magnetic property of the samples was measured with a magnetic property measurement system (MPMS 7 T, Quantum Design). The strain-electric-field measurement was carried out using an optical probe system (SIOS NT-04 Sensor).

The XRD pattern of the PCMO/PMN-PT heterostructure shown in Fig. 1(a) indicates that PCMO is single phase with a c-axis orientation. The c-axis lattice constant of the PCMO film is calculated to be 0.3807 nm, which is smaller than 0.3832 nm of the PCMO bulk.¹⁴ So the substrate-induced

^{a)}Electronic mail: ygzhao@tsinghua.edu.cn.

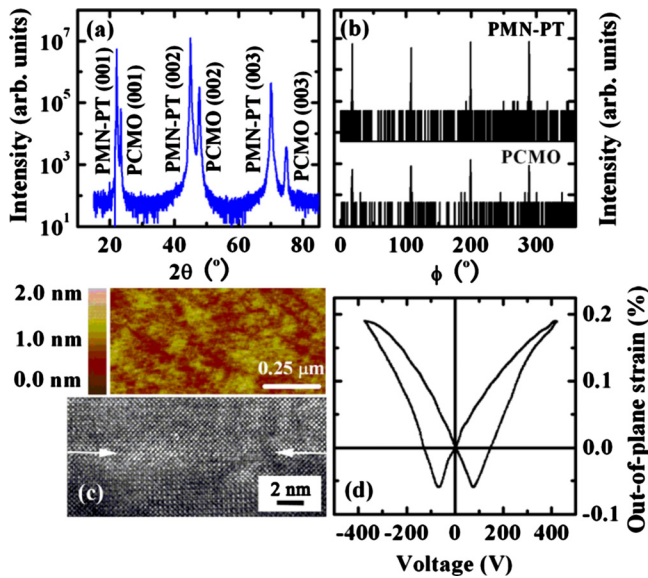


FIG. 1. (Color online) (a) XRD pattern for PCMO/PMN-PT. (b) ϕ scan for PCMO and PMN-PT, respectively. (c) The upper panel is the surface morphology of PCMO film. The lower panel is the TEM cross-sectional image of PCMO/PMN-PT. (d) Out-of-plane piezostrain vs electric field $E_{\parallel}(001)$.

strain is compressive along the out-of-plane direction (-0.65%) and tensile along the in-plane direction. Figure 1(b) is the ϕ scan result for the PCMO film and PMN-PT substrate, which indicates an epitaxial growth of PCMO on PMN-PT. The epitaxial growth of PCMO is also demonstrated by the TEM cross-sectional image of PCMO/PMN-PT shown in the lower panel of Fig. 1(c). The upper panel of Fig. 1(c) shows the surface morphology of the PCMO film and the calculated root-mean-square roughness of the film is 0.525 nm. Figure 1(d) is the variation in the out-of-plane strain with applied electric field for PMN-PT, which shows a butterfly behavior with a coercive field of 1.6 kV/cm.

Figure 2(a) is the magnetic hysteresis of PCMO measured at 30 K between -7.0 and 7.0 T after a zero magnetic field cooling (ZFC). Unlike the conventional FM, the initial magnetization curve of PCMO does not lie between the field descending and ascending curves of the hysteresis loop but below the hysteresis loop. This result is consistent with a metamagnetic transition from COAFM to FM and its memory effect which has also been observed in other phased separated manganites.¹⁵ The lower inset of Fig. 2(a) shows a divergence between the ZFC and the magnetic field cooling (FC, 500 Oe) curves, which is consistent with the previous report.¹⁶

The PMN-PT substrate was first poled with an electric field of 8.0 kV/cm at 400 K and then the temperature dependence of magnetizations [$M(T)$] were measured in a FC (500 Oe) process under different electric fields. The upper inset of Fig. 2(a) is the scheme of the sample. The results for the in-plane $M(T)$ are shown in Fig. 2(b), which reveals dramatic increase in magnetization with increasing electric field below the FM transition temperature (120 K). The increase in the in-plane magnetization can reach 60% for $\Delta M/M(0)$ at 8.0 kV/cm (400 V) [$\Delta M = M(E) - M(0)$, where $M(E)$ and $M(0)$ are the magnetizations with and without an electric field, respectively]. In order to understand the mechanism of the electric-field control of magnetization, the magnetic hysteresis loops of the sample were measured for both the in-plane and out-of-plane directions and the results are shown in Figs. 2(c) and 2(d). The sample was first cooled to 30 K in a ZFC process under different electric fields and the magnetic hysteresis loops of the sample were measured with the applied cooling electric fields. It can be seen that both the out-of-plane and in-plane magnetizations increase with applied electric field. The magnetizations for different in-plane directions also increase with applied electric field (not shown here). The results suggest that the electric-field control of magnetization in PCMO/PMN-PT is dominated by the change in magnetic anisotropy for which opposite changes for the in-plane and out-of-plane directions are expected.⁶

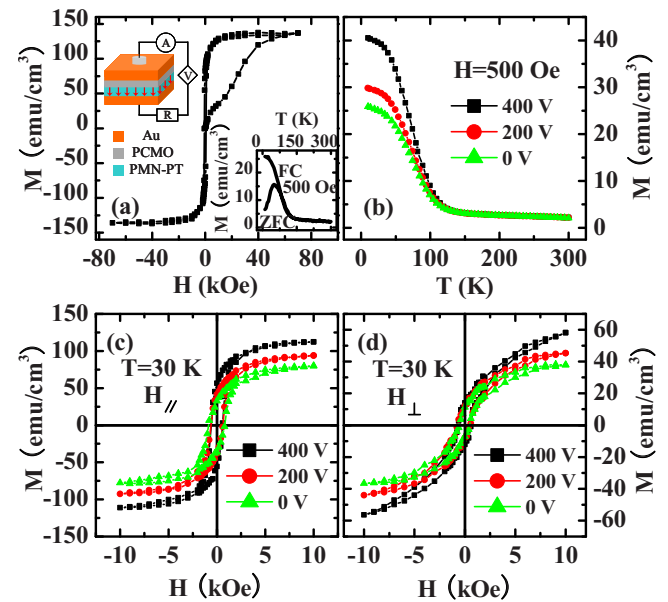


FIG. 2. (Color online) (a) Magnetic hysteresis of PCMO at 10 K. The upper inset is the scheme of the sample. The lower inset is the FC and ZFC curves. (b) Temperature dependence of the in-plane magnetization under different electric fields. [(c) and (d)] Magnetic hysteresis loops under different electric fields for the (c) in-plane and (d) out-of-plane directions.

It is well-known that phase separation in manganites can be tuned by various factors with a memory effect.¹⁰ However, so far there is no report on the memory effect of strain in the phase separated manganites. Figure 3(a) is the mag-

netic hysteresis loops in a ZFC process with 0 , 300 V cooling and the removal of the voltage. The inset is the temperature dependence of the recovery ratio. (b) The curves with \blacktriangle and \blacksquare symbols are $M(T)$ with 500 Oe and 300 V cooling and warming after the removal of the magnetic and electric fields. The curves with \triangle and \square symbols are $M(T)$ with 1550 Oe cooling and warming after the removal of 1550 Oe. Inset: the black curve is 300 V cooling and 300 V warming and the green curve is 300 V cooling and 0 V warming.

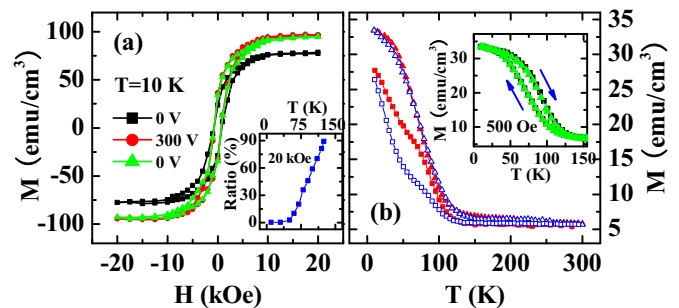


FIG. 3. (Color online) (a) Magnetic hysteresis loops in a ZFC process with 0 , 300 V cooling and the removal of the voltage. The inset is the temperature dependence of the recovery ratio. (b) The curves with \blacktriangle and \blacksquare symbols are $M(T)$ with 500 Oe and 300 V cooling and warming after the removal of the magnetic and electric fields. The curves with \triangle and \square symbols are $M(T)$ with 1550 Oe cooling and warming after the removal of 1550 Oe. Inset: the black curve is 300 V cooling and 300 V warming and the green curve is 300 V cooling and 0 V warming.

netic hysteresis loops of the sample measured at 10 K after ZFC with (red curve) and without (black curve) an electric field. After the measurement of the magnetic hysteresis loop at an electric field of 6.0 kV/cm (300 V, red curve), the electric field was removed *in situ* and then the magnetic hysteresis loop (green curve) was measured after about 500 s. It can be seen that the magnetization remains nearly unchanged after the removal of the electric field (strain), manifesting a memory effect of strain in PCMO. Similar measurements were also carried out at other temperatures. The temperature dependence of the recovery ratio, defined as $(M_E - M_{E0}) / (M_E - M_0)$, where M_0 , M_E , and M_{E0} are the magnetizations of the black, red, and green curves, respectively, was calculated from these magnetic hysteresis loops at $H = 20$ kOe and the result is shown in the inset of Fig. 3(a). It shows that the recovery ratio starts to increase rapidly at about 50 K with increasing temperature. This indicates that the memory effect is robust below 50 K and becomes weak with increasing temperature. We also studied the memory effect by measuring the $M(T)$ curves and the results are shown in the inset of Fig. 3(b). The cooling curves were first measured in a FC (500 Oe) process at an electric field of 6.0 kV/cm (300 V). The warming curves were measured in a magnetic field warming (FCW, 500 Oe) process with (black curve) and without (green curve) the electric field, respectively. It can be seen that the two curves of FCW process coincide, manifesting a memory effect. The FC curve and FCW curve exhibit a thermal hysteresis behavior, consistent with a first-order phase transition. It is also interesting to compare the effects of the magnetic and electric fields by measuring the temperature dependence of the magnetization and the results are shown in Fig. 3(b). The curve with solid triangles was obtained in a FC (500 Oe) process at 6.0 kV/cm while the curve with open triangles was obtained in a FC (1550 Oe) process without an electric field. These two curves are almost overlapped indicating that the increase in the magnetization induced by an electric field of 6.0 kV/cm approximately equals to the effect of a magnetic field of 1050 Oe. However, after removing both the magnetic and electric fields at 10 K and measure the magnetization with increasing temperature, the curve with solid squares is above the curve with open squares. This difference can be understood by considering that the electric field changes the phase separation in PCMO with a memory effect while the magnetic field changes the orientation of magnetic domains besides the phase separation in PCMO and the magnetic domains tend to change the orientation after the removal of the magnetic field.

The electric-field control of magnetization in the PCMO/PMN-PT heterostructures can be understood in terms of the electric-field-induced strain in the PCMO films. The out-of-plane and in-plane strains in PMN-PT satisfy $\varepsilon_{zz} = -2\nu / (1 - \nu) \varepsilon_{xx}$,¹⁷ where ε_{zz} , ε_{xx} , and ν are the out-of-plane strain, in-plane strain, and Poisson coefficient, respectively. In a first-order approximation, one can assume volume conservation corresponding to $\nu = 0.5$, which results in $\varepsilon_{xx} = \varepsilon_{yy} = -1/2 \varepsilon_{zz}$. Using the data of ε_{zz} in Fig. 1(d), the in-plane strains can be calculated. For example, the values of ε_{xx} are about 0 (0 V), -0.05% (200 V), and -0.10% (400 V). Ahn *et al.*¹⁸ proposed a model to account for the phase separation

in manganites by considering the elastic energy that gives rise to an energy landscape with multiple energy minima. In this scenario, the strain in manganites determines the energy landscape. This model can explain our results. The PCMO/PMN-PT heterostructure was cooled down under different strains, which lead to the different energy landscapes with hierarchical energy barriers. The in-plane strains are negative as shown above and tend to weaken the tensile strain in the as-grown PCMO, which favors the FM phase due to the weakening of Jahn–Teller distortion. This leads to the dramatic increase in magnetization. Since the FM and COAFM phases correspond to two local minima in the free energy with a potential barrier separating them,¹⁹ at low temperatures, the magnetization of the sample does not change after the removal of the electric field (strain) because the thermal energy is too small to overcome the barrier to drive the sample to the strain-free state, manifesting a memory effect of strain.

This work was supported by the 973 project (Grant No. 2009CB929202), National Science Foundation of China (Grant Nos. 50872065, 50772054, and U0734001), and Tsinghua National Laboratory for Information Science and Technology (TNList) Cross-discipline Foundation. This work made use of the resources of the Beijing National Center for Electron Microscopy.

- ¹For recent review, see C. A. F. Vaz, J. Hoffman, C. H. Ahn, and R. Ramesh, *Adv. Mater. (Weinheim, Ger.)* **22**, 2900 (2010); J. Ma, J. M. Hu, Z. Li, and C. W. Nan, *ibid.* **23**, 1062 (2011).
- ²W. Eerenstein, M. Wiora, J. L. Prieto, J. F. Scott, and N. D. Mathur, *Nature Mater.* **6**, 348 (2007).
- ³C. Thiele, K. Dörr, O. Bilani, J. Rödel, and L. Schultz, *Phys. Rev. B* **75**, 054408 (2007).
- ⁴H. F. Tian, T. L. Qu, L. B. Luo, J. J. Yang, S. M. Guo, H. Y. Zhang, Y. G. Zhao, and J. Q. Li, *Appl. Phys. Lett.* **92**, 063507 (2008).
- ⁵Y. Chen, J. Wang, M. Liu, J. Lou, N. X. Sun, C. Vittoria, and V. G. Harris, *Appl. Phys. Lett.* **93**, 112502 (2008).
- ⁶J. J. Yang, Y. G. Zhao, H. F. Tian, L. B. Luo, H. Y. Zhang, Y. J. He, and H. S. Luo, *Appl. Phys. Lett.* **94**, 212504 (2009).
- ⁷Y. Zhang, J. Liu, X. H. Xiao, T. C. Peng, C. Z. Jiang, Y. H. Lin, and C. W. Nan, *J. Phys. D: Appl. Phys.* **43**, 082002 (2010).
- ⁸M. C. Dekker, A. D. Rata, K. Boldyreva, S. Oswald, L. Schultz, and K. Dörr, *Phys. Rev. B* **80**, 144402 (2009).
- ⁹Z. G. Sheng, J. Gao, and Y. P. Sun, *Phys. Rev. B* **79**, 174437 (2009).
- ¹⁰E. Dagotto, *Nanoscale Phase Separation and Colossal Magnetoresistance* (Springer, Berlin, 2003).
- ¹¹Y. Tomioka, A. Asamitsu, H. Kuwahara, Y. Moritomo, and Y. Tokura, *Phys. Rev. B* **53**, R1689 (1996).
- ¹²W. Prellier, E. Rauwel Buzin, Ch. Simon, B. Mercey, and M. Hervieu, *Phys. Rev. B* **66**, 024432 (2002).
- ¹³T. Wu, S. B. Ogale, S. R. Shinde, A. Biswas, T. Polletto, R. L. Greene, and T. Venkatesan, *J. Appl. Phys.* **93**, 5507 (2003).
- ¹⁴C. S. Nelson, J. P. Hill, D. Gibbs, M. Rajeswari, A. Biswas, S. Shinde, R. L. Greene, T. Venkatesan, A. J. Millis, F. Yokaichiya, C. Giles, D. Casa, C. T. Venkataraman, and T. Gog, *J. Phys.: Condens. Matter* **16**, 13 (2004).
- ¹⁵W. Wu, C. Israel, N. Hur, S. Park, S.-W. Cheong, and A. De Lozanne, *Nature Mater.* **5**, 881 (2006).
- ¹⁶T. Mertelj, R. Yuzupov, M. Filippi, W. Prellier, and D. Mihailovic, *Appl. Phys. Lett.* **93**, 042512 (2008).
- ¹⁷R. K. Zheng, C. Chao, H. L. W. Chan, C. L. Choy, and H. S. Luo, *Phys. Rev. B* **75**, 024110 (2007).
- ¹⁸K. H. Ahn, T. Lookman, and A. R. Bishop, *Nature (London)* **428**, 401 (2004).
- ¹⁹J. López, W. P. N. Lisboa-Filho, W. A. C. Passos, W. A. Ortiz, F. M. Araujo-Moreira, O. F. de Lima, D. Schaniel, and K. Ghosh, *Phys. Rev. B* **63**, 224422 (2001).